Tectonophysics 691 (2016) 282–289

Contents lists available at ScienceDirect

Tectonophysics

journal homepage: www.elsevier.com/locate/tecto

Serpentinization of the fore-arc mantle along the Taiwan arc-continent collision of the northern Manila subduction zone inferred from gravity modeling

Wen-Bin Doo [a,*], Hao Kuo-Chen [b], Dennis Brown [c], Chung-Liang Lo [b], Shu-Kun Hsu [a,b], Yin-Sheng Huang [a]

[a] Center for Environmental Studies, National Central University, Taiwan
[b] Department of Earth Sciences, National Central University, Taiwan
[c] Institute of Earth Science "Jaume Almera", CSIC, Barcelona E-08028, Spain

ARTICLE INFO

Article history:
Received 13 June 2016
Received in revised form 6 October 2016
Accepted 18 October 2016
Available online 20 October 2016

Keywords:
Serpentinization
Exhumation
Gravity modeling
Taiwan orogen

ABSTRACT

Serpentinized peridotite in the fore-arc has been observed in a number of subduction zones, including the northern Manila subduction zone which terminates northward in the Taiwan arc-continent collision. How this zone of serpentinization changes northward from the subduction of thinned continental lithosphere to full arc-continent collision in the Taiwan orogeny is not well known. In this paper we present 2-D gravity modeling along three P-wave (Vp) transects across the Taiwan orogeny. Two of these transects were collected with ocean-bottom seismometers. These two transects provide good constraints on the velocity structure to the west of, and on land, southern Taiwan. Conversion of Vp to density in this area allows us to model the gravity anomaly with very little misfit. Along the subduction zone, however, the velocity models are poorly constrained in the upper mantle, where an anomalous density unit has to be used in order to model the short wavelength gravity anomaly in this area. A third transect across central Taiwan that is derived from the TAIGER local tomography data, provides good control on the crust and upper mantle Vp structure that we use to place provide density constraints for modeling the gravity anomaly in this part of the collision zone. In order to model the short wavelength gravity anomaly across the Longitudinal Valley and the southern Longitudinal trough, an anomalous density block is required beneath the fore-arc region. We interpret that the source of this anomalous density material could be serpentinized fore-arc mantle, similar to what is interpreted for the northern Manila subduction zone farther south. Water released from the subduction of the extended crust of the continental margin results in the serpentinization of the fore-arc area and may be driving the uplifting of the high-pressure rocks.

1. Introduction

A wide range of geophysical and geological data indicate that serpentinization of the fore-arc mantle wedge is a common feature of many subduction zones worldwide (Bostock et al. 2002; Hyndman and Peacock 2003). To identify serpentinization in the fore-arc mantle region of subduction zones, velocity and density modeling provide useful tools for determining both the presence and the amount of serpentine that is present (e.g., Xia et al. 2015; Zhao 2012; Hacker et al., 2003). This is aided by laboratory measurements that illustrate a significant reduction in the seismic velocity and density of peridotite with an increase in the modal abundance of serpentine (Christensen 1966, 2004; Horen et al. 1996; Hyndman and Peacock 2003) (Fig. 1).

In the northern Manila subduction zone, where the thinned continental crust of the Eurasia Plate (EUP) margin is subducting below the northern Luzon arc on the Philippine Sea Plate (PSP), forward gravity modeling along two TAIGER transects (T1 and T2) led Doo et al. (2015) to interpret an area of relatively high density materials in the fore-arc region. The relatively higher density of this area compared to the overlying fore-arc and its lower density compared to the adjacent mantle led Doo et al. (2015) to interpret this observation as a partly serpentinized mantle that is being exhumed along the subduction interface. Farther north, where the full thickness of the continental crust is now in the subduction zone (Chen et al. 2004; Lin 2009), an area of relatively high Vp below the fore-arc has also been interpreted to be serpentinized mantle (Van Avendonk et al. 2014) or a combination of this lithology and mafic eclogite that are being exhumed along the subduction zone (Brown et al. 2015). This area of high Vp is also marked by a short wavelength low in the free-air anomaly that extends from the northern part of the Longitudinal Valley into the southern Longitudinal trough offshore southeast Taiwan (Fig. 2). 2D forward gravity modeling across the Taiwan arc-continent collision adds new constraints to the interpretation of the material in the fore-arc region that

* Corresponding author.
E-mail address: wenbindoo@gmail.com (W.-B. Doo).

http://dx.doi.org/10.1016/j.tecto.2016.10.019
0040-1951/

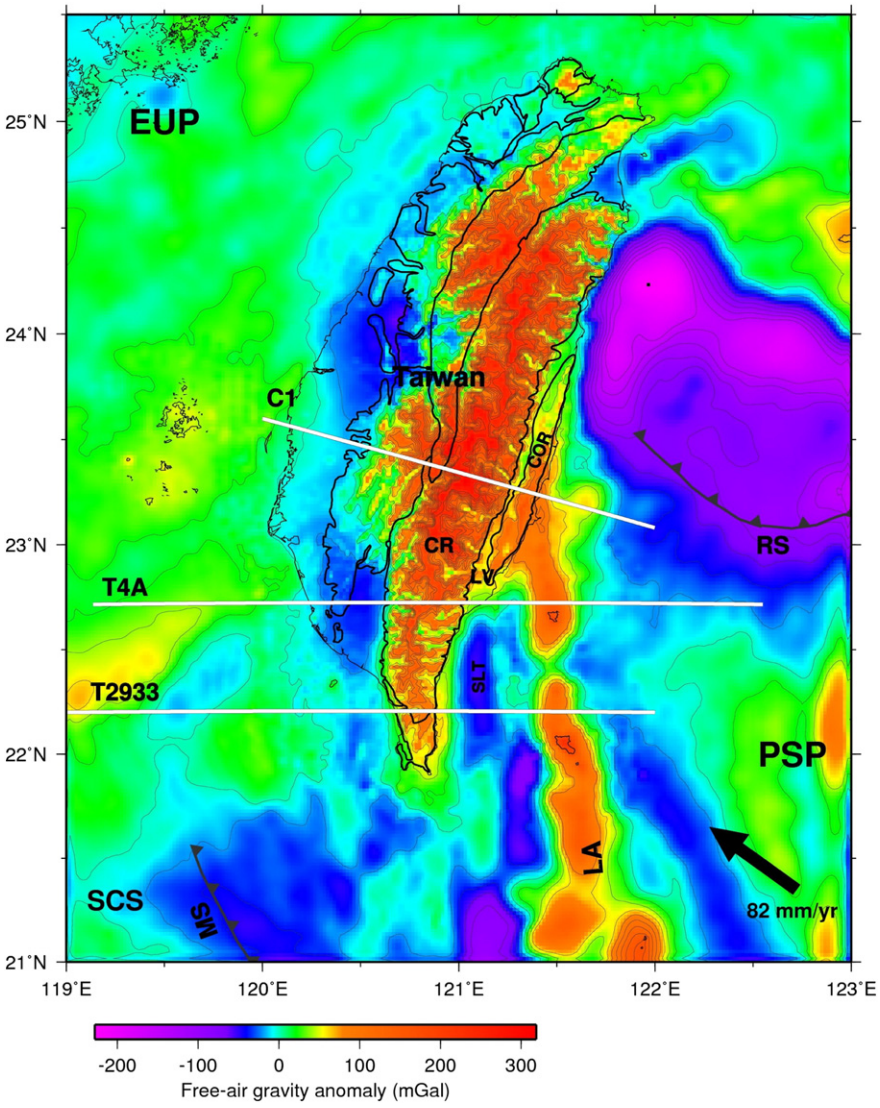

Fig. 1. Free-air gravity anomaly map (Hwang et al. 2014) of the Taiwan region. The black arrow indicates the relative plate motion. The locations of 2-D gravity modeling transects shown in Figs. 2, 3 and 4 are indicated by thick white lines labeled T2933, T4A and C1. Abbreviations - CR: Central Range; COR: Coastal Range; EUP: Eurasia Plate; LA: Luzon arc; LV: Longitudinal Valley; MS: Manila subduction zone; RS: Ryukyu subduction zone; PSP: Philippine Sea Plate; SLT: southern Longitudinal trough; SCS: South China Sea.

is causing this low and strengthens the interpretations based on the velocity structure.

In this paper we present the results of 2-D gravity modeling along three velocity transects that cross the central and southern Taiwan (Fig. 2) with the goals of better constraining the shallow lithological structure of the fore-arc region in eastern Taiwan and subsequently investigating the possible implications of serpentinite in the exhumation of mantle and high-pressure rocks from the northern Manila subduction zone to the Taiwan arc-continent collision.

2. Tectonic background

The Taiwan orogen is forming as a result of the subduction of the EUP continental margin beneath the Luzon arc on the PSP along the northernmost part of the Manila Subduction zone (Fig. 1). The convergence between these two plates is roughly northwestward. Of interest to this paper, the contact between the two colliding plates in eastern Taiwan is a zone of oblique faulting, with the exhumation of high-pressure rocks, parts of the volcanic arc, and partially serpentinized mantle taking place since the Late Miocene (Beyssac et al. 2008). In the geophysical data sets, this is marked by a velocity high that extends eastward to at least 50 km beneath the Luzon arc (Huang et al. 2014). A tight clustering of seismicity is observed along the upper margin of this velocity high that extends to the Moho beneath the arc. In addition, a short wavelength gravity low is found across this area. Modeling this low can provide further insights into the possible composition of the rocks along the shallow part of the subduction interface as well as the processes occurring there.

A number of studies have used either active-source or earthquake seismic data to produce P-wave seismic velocity images of Taiwan and its surrounding oceans (Hetland and Wu 1998; Kim et al. 2006; McIntosh et al. 2005; Wu et al. 2007; Kuo-Chen et al. 2012; Huang et al. 2014). Several tomography studies (Lin et al. 1998; Kuo-Chen et al. 2012; Van Avendonk et al. 2014; Huang et al. 2014) have shown that there is a high-velocity zone present in the crust of the Central Range and in the crust and upper mantle beneath the Luzon arc. Lin et al. (1998) and Lin (2002) interpreted these high-velocity zones to be the same feature and to be related to crustal exhumation. This feature was interpreted by McIntosh et al. (2013) to be accreted transitional crust (ATC) within the Central Range of the orogen. However, due to poor resolution of the velocity model in the deeper part of the Central Range and fore-arc region, McIntosh et al. (2013) could not interpret the structure in these areas. In other interpretations, Cheng (2009), for example, found two prominent high-velocity areas in the middle to lower crust

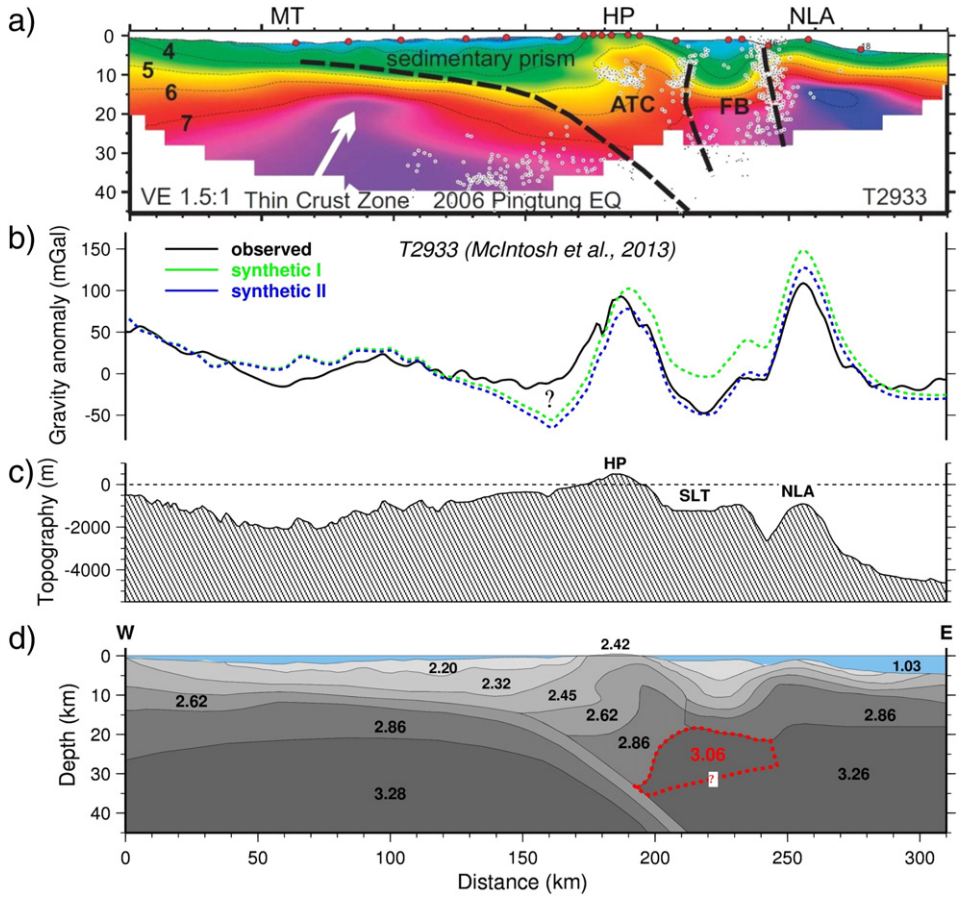

Fig. 2. 2-D gravity modeling of the transect T2933 across south Taiwan. The profile location is shown in Fig. 2. (a) Velocity structures along the profile (modified from McIntosh et al. 2013). The black dashed line indicates basal detachment between the accretionary prism and subducting continental crust. (b) Observed (Hwang et al. 2014) and synthetic gravity anomalies. Synthetic I is the result of the slightly revised density model. Synthetic II an anomalous-density unit (red block) is placed in the fore-arc region. (c) Topography variation along the profile and (d) gravity modeling result. ATC: accreted transitional crust; CR: Central Range; FB: fore-arc block; HP: Hengchun peninsula; MT: Manila Trench; NLA: North Luzon Arc; SLT: southern Longitudinal trough.

beneath the offshore area (interpreted as the LA and fore-arc blocks) and the upper to middle crust beneath the Central Range (interpreted as uplift material from the oceanic crust scraped from the Luzon fore-arc). More recently, Van Avendonk et al. (2014), using TAIGER transect T5, which crossed eastern Taiwan where the Ryukyu subduction zone interacts with it, interpreted the presence of serpentinized mantle rocks beneath eastern Taiwan to explain their observations. Furthermore, Brown et al. (2015) used petrophysical modeling of the high-velocity zone to suggest that the deeper part of the may be comprised of serpentinized mantle rock types and/or mafic eclogite.

3. Gravity and seismic velocity data of central and south Taiwan

In recent years two international experiments have been carried out to explore the geological processes taking place in the deep crust and upper mantle of the Taiwan arc-continent collision: TAICRUST, which was carried out in 1995, and the TAIGER projects, which were carried out in 2009. In this study, we use transects T2933 and T4A from the TAICRUST and TAIGER experiments and transect (C1) taken from the TAIGER local tomography model of Kuo-Chen et al. (2012). Transects T2933 and T4A were acquired using ocean-bottom seismometers (OBS) data offshore and land instruments that cross southern Taiwan (Fig. 1). Both transects show that the hyper-extended continental crust of the Chinese continental margin is subducting at the Manila Trench (Figs. 2a and 3a) and that a high-velocity rise exists roughly between km 200–240. These data provide good constraints on the P-wave velocity structure of the crust (McIntosh et al. 2013); however, because of resolution problems, they do not provide clear images of the deeper structure, especially along the subduction zone in eastern Taiwan. Profile C1, across central Taiwan, provides a P-wave velocity structural image that clearly reveals the high velocity zone that extends eastward beneath the Luzon arc. Newly obtained gravity anomaly data around Taiwan have been compiled by Hwang et al. (2014). This dataset enhances data resolution onland in Taiwan. In the 2D gravity modeling that follows we use these Vp profiles to place constraints on the density structure of the crust and upper mantle.

4. Gravity modeling

Gravity modeling was carried out by converting the P-wave velocity models for transects T2933 and T4A and transect C1 (Figs. 2a, 3a, 4a) using the P-wave to density Eq. 1 of Brocher (2005).

$$\rho(\mathrm{g/cm^3}) = 1.6612V_p - 0.4721V_p^2 + 0.067V_p^3 - 0.0043V_p^4 + 0.000106V_p^5 \quad (1)$$

This equation is valid for Vp between 1.5 and 8.5 km/s. We first constructed the layer geometries according to the velocity contours. In areas where the resolution of the velocity models area poor, we extended the velocity contours smoothly to be the layer boundaries and then adjusted the densities until the synthetic anomaly was fitted to the measured gravity anomaly (Figs. 2 to 4). For example, we selected the Vp velocity 5.0 and 6.0 km/s contour lines to be the top and bottom depths of the upper-crust, respectively. Thus, the initial density of this block is 2.62 g/cm^3 (average Vp = 5.5 km/s) according to Eq. 1. Next,

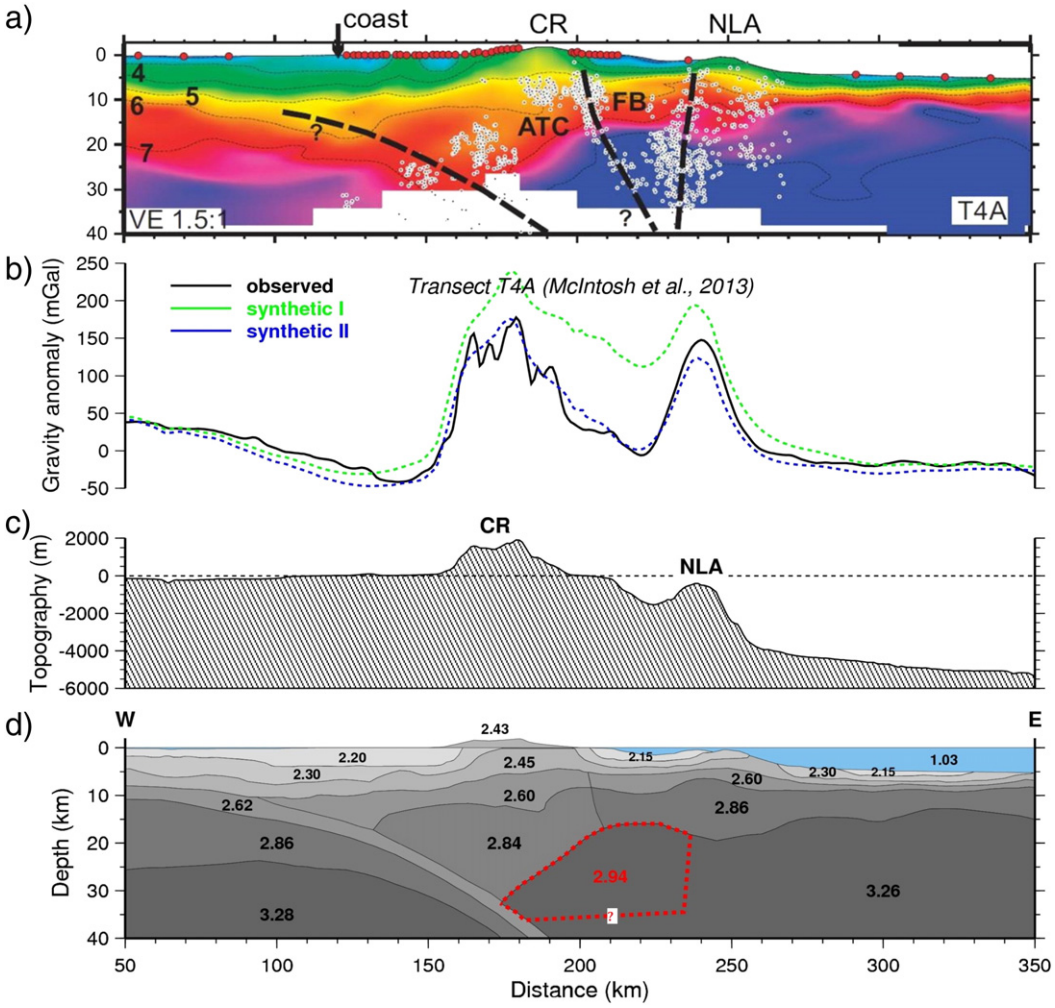

Fig. 3. 2-D gravity modeling of the transect T4A across south Taiwan. The profile location is shown in Fig. 2. (a) Velocity structures along the profile (modified from McIntosh et al. 2013). (b) Observed (Hwang et al. 2014) and synthetic gravity anomalies. Synthetic I is the result of the slightly revised density model. Synthetic II an anomalous-density unit (red block) is placed in the fore-arc region. (c) Topography variation along the profile and (d) gravity modeling result. ATC: accreted transitional crust; CR: Central Range; FB: fore-arc block; NLA: North Luzon Arc.

to fit the observed gravity anomaly, we slightly adjusted this density (we allow ± 1.5% density variation for each layer). Although the gravity modeling is non-unique, the constraints placed crustal structure, and hence the densities of the gravity model, help to reduce the non-uniqueness of the model. This, then, provides possible solutions for the structure of the deeper fore-arc area that is poorly resolved in the velocity models. In Figs. 2 and 3, the density models are roughly the same (layering and its relative density). Synthetic model I is the result of a slightly revised density model (considering the material of the red block is normal mantle), whereas in synthetic model II, an anomalous-density unit (red block) is placed in the fore-arc region.

Overall, our density models coincide very well with the velocity models. We find that if there is no anomalous density material presented in the fore-arc region, then the maximum misfit between synthetic model I (green dashed line shown in Figs. 3 and 4) and the observed gravity anomalies (Hwang et al. 2014) can reach 40 and 130 mGal in transects T2933 and T4A, respectively. To achieve make a better fit with the observed gravity data, in synthetic model II, areas with a density of 3.06 and 2.94 g/cm^3 for transects T2933 and T4 A, respectively, have been added. In profile C1, if the high velocity zone beneath the fore-arc region, between km 135–153 (Fig. 4) does not exist, then a maximum misfit occurs between synthetic model I (green dashed line shown in Fig. 5) and the observed gravity anomaly of up to 55 mGal. To reduce this misfit, in synthetic model II, a high-density (high seismic velocity) material of 3.16 g/cm^3 is necessary (Fig. 4). This suggests that rocks present in this part of the fore-arc must have densities that are higher than those for the average continental crust that is subducting and lower than that for the average mantle peridotite beneath the Luzon arc.

5. Discussion

Because of the arc-continental collision, the slab dip becomes steeper from south to central Taiwan (Kuo-Chen et al. 2012). The Moho depth from the receiver function reveals a typical continental crust of 30 km in western Taiwan and becomes thicker eastward to the Central Range (53 km) (Wang et al. 2010). One of the key questions that we seek to address in this paper is how this anomalous zone in the velocity and density structure of the fore-arc region changes northward as increasingly thicker continental crust enters the subduction zone. Using forward gravity modeling along transects T1 and T2 (Fig. 5) farther south, where the thinned continental crust is being subducted, Doo et al. (2015) found that a relatively high density material must be present in the fore-arc region to fit the observed free-air gravity anomaly. They interpreted this relatively high density material to be serpentinized mantle peridotite in the fore-arc region. The pronounced short wavelength low in the free-air gravity anomaly across the fore-arc region modeled by Doo et al. (2015) continues northward in the southern

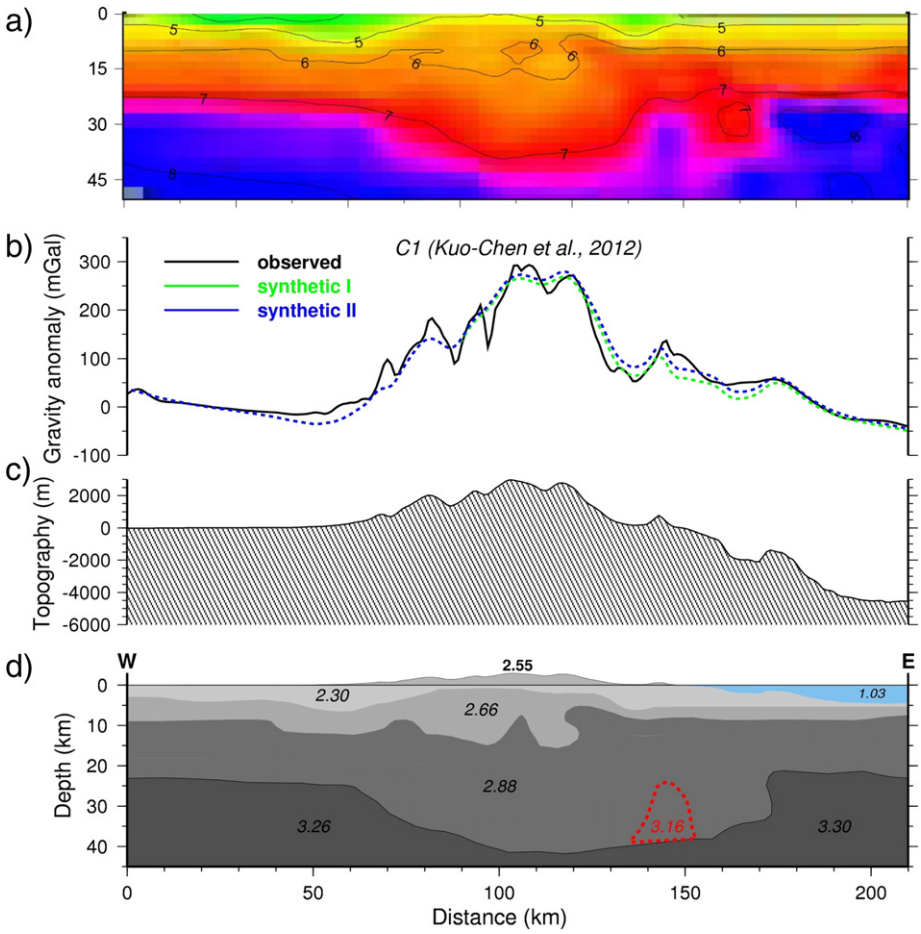

Fig. 4. 2-D gravity modeling of the profile C1 across central Taiwan. The profile location is shown in Fig. 2. (a) Velocity structures along the profile (Kuo-Chen et al. 2012). (b) Observed (Hwang et al. 2014) and synthetic gravity anomalies. Synthetic I considering the density of the red block is 2.88 g/cm^3. Synthetic II is the result of the direct conversion Vp to density. (c) Topography variation along the profile and (d) gravity modeling result.

Longitudinal trough to the southeast of Taiwan (Fig. 5). Here, in transects T2933 and T4A, this low gravity can be modeled with a density of 3 g/cm^3 ($\pm$0.06). This anomalous density block is found only in the fore-arc region, at a depth of between 15–35 km. Considering the density and the location of this block, we interpret the source of this anomalous density material to be the serpentinized mantle.

In the case of C1, where the full thickness of the continental crust is now in the collision zone, the density required to fit the free-air gravity anomaly in eastern Taiwan is 3.16 g/cm^3. Because of the appropriate geometry of this block, we can estimate the degree of serpentinization from the density variation. On average, unaltered peridotite with a density of about 3.29 g/cm^3 (Christensen 1966) indicates that these rocks have undergone approximately 18% serpentinization. Alternatively, the Vp velocity (7.5 km/s) of this block could represent a level of serpentinization of approximately 24% (Christensen 1966). This is in accordance with petrophysical analyses of the high-velocity zone in eastern Taiwan performed by Brown et al. (2015), who showed that a number of possible rock types can fit the velocity structure; however, if mantle rocks are present, they must be partly serpentinized. They showed that the degree of serpentinization decreases with depth: at 20 km depth, mantle rock types with 20%–30% serpentinization fit the velocity structure, whereas at 30 km and deeper only 10% to 20% serpentinization is required.

The red bodies in transects T1 and T2 (Fig. 5b) have a completely different location than the other transects (T2933, T4A and C1) we presented in this study (Fig. 5). It is interesting and important. Here, we provide a possible reason to explain it. In the case of weak plate coupling status, the overriding plate is detached from the subducted plate, and then asthenospheric material can upwell into the plate contact zone (Gvirtzman and Nur 1999). In the northern Manila subduction zone, because of the weak plate coupling status (Lo et al. 2015), plate detachment can yield space, and then positive buoyancy force leads the serpentinized materials to be uplifted to the plate contact zone automatically. The gravity modeling for transects T1 and T2 from Doo et al. (2015) have demonstrated this phenomenon (Fig. 5). Thus, weak plate coupling status and positive buoyancy are the main factors to cause the serpentinized materials uplifting in the northern Manila subduction zone.

Gravity modeling results (Figs. 2 to 4) reveal that the serpentinized materials are roughly located beneath the Longitudinal Valley and its southward extending region (southern Longitudinal trough) (Fig. 5). Onland Taiwan, a rifted continental margin that was accreted in the early stage of the collision formed a new backstop. The collision of the EUP continental crust with overriding Luzon arc formed a broad crustal root beneath central Taiwan, possibly with a thickness of 55 km (Kuo-Chen et al. 2012; Van Avendonk et al. 2014). Thickening of the Central Range crust results in the relatively low density crustal materials going down and not only resisting serpentinized materials to uplift but also compressing the underlying serpentinized materials, leading these materials to move laterally. Simultaneously, the creation of the Coastal Range and its root occur when the PSP and the EUP are colliding while the PSP subducts to the north (Kao and Jian 2001; Wu et al. 2009). Furthermore, the serpentinization process can reduce the mechanical strength of the rocks (Hyndman and Peacock 2003). Between the PSP

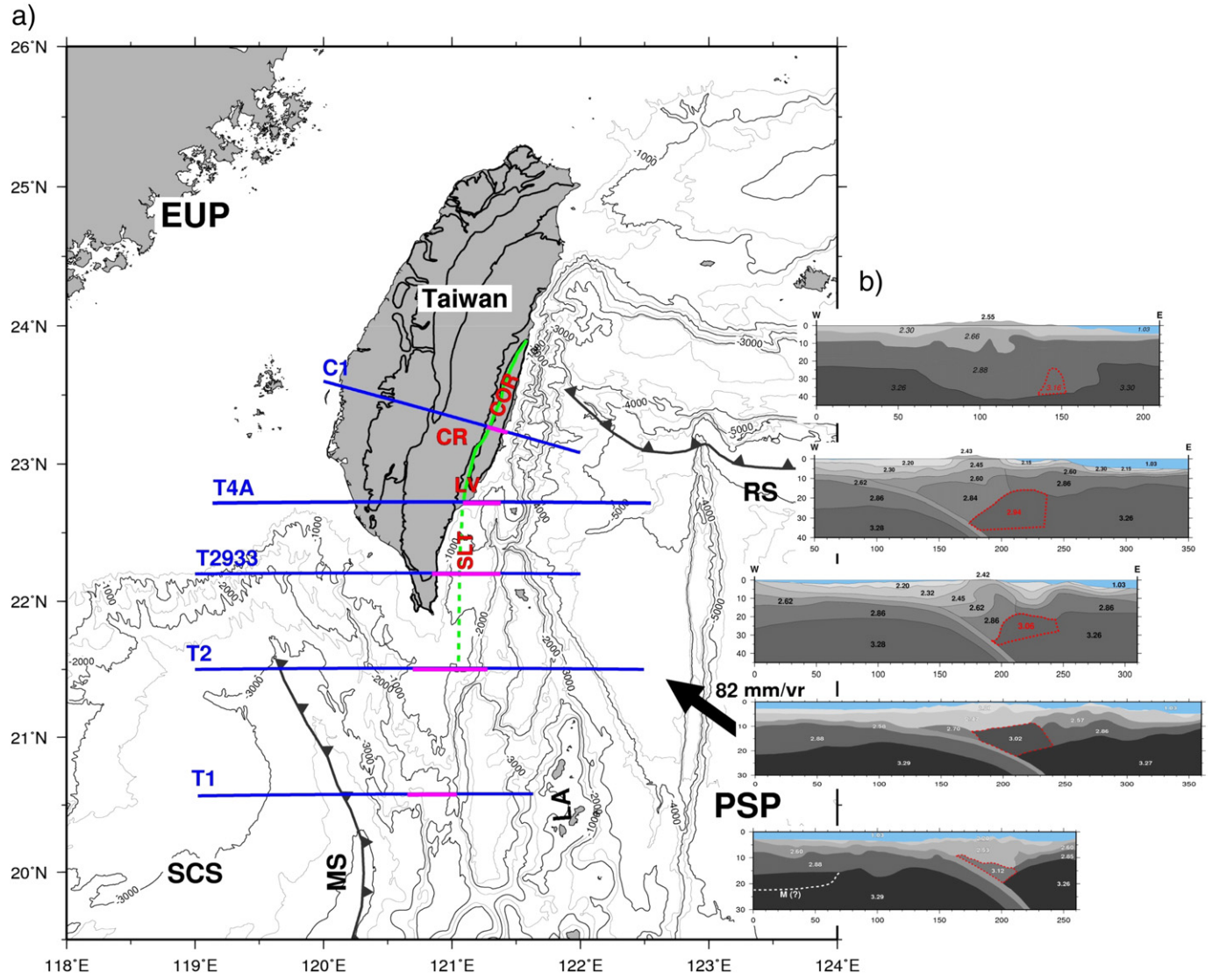

Fig. 5. (a) Overview map of the Taiwan region. The locations of 2-D gravity modeling transects are indicated by thick blue lines. Pink lines indicate the distributions of serpentinized materials. Thick black lines indicate the boundary of different tectonistratigraphic unit. (b) Density structure of the 2-D gravity modeling transects. Abbreviations - CR: Central Range; COR: Coastal Range; EUP: Eurasia Plate; LA: Luzon arc; LV: Longitudinal Valley; MS: Manila subduction zone; RS: Ryukyu subduction zone; PSP: Philippine Sea Plate; SLT: southern Longitudinal trough; SCS: South China Sea.

and the EUP, the Longitudinal Valley indicates the suture zone, i.e., a zone of weakness that is hence easy to deform. Geodetic data show 82 mm/yr of NW-SE convergence between the PSP and EUP at present (Yu et al., 1997). In eastern Taiwan, approximately 30–40 mm/yr of this convergence is accommodated near the Longitudinal Valley (Yu and Kuo 2001) between the Coastal Range and the Central Range. The deformation may be a direct result of convergence. Thus, we interpret that the initial distribution of serpentinized materials could be wider (deeper part), caused by the dehydration of the subducting EUP. Compressional force results in the serpentinization materials being constrained and rising along the Longitudinal Valley, i.e., the suture zone. In addition, the velocity model of Kuo-Chen et al. (2012) also revealed a clear image of high-velocity rise under the Longitudinal Valley between the Central Range and the Coastal Range (Fig. 6). The 2-D gravity modeling results are consistent with their result.

6. Conclusion

In all transects (T2933, T4A and C1) we found that anomalous density blocks are needed to fit the observed gravity anomaly (Hwang et al. 2014). According to the characteristics of serpentinization and the formation of serpentinized fore-arc mantle, we interpret the source of this anomalous density material as the serpentinized mantle rocks. The degree of serpentinization could be about 18% for transect C1. The serpentinized peridotite onland Taiwan is roughly constrained along the Longitudinal Valley, i.e., the suture zone, between the PSP and the EUP.

Geological studies combined with numerical modeling have shown that serpentinization of the fore-arc mantle plays an important role in the uplifting of high-pressure terranes along subduction zones (Gerya et al. 2002; Gerya 2011; Hacker and Gerya 2013; Erdman and Lee 2014). In this study, we proposed that the major mechanisms causing the uplifting of serpentinized materials in the subduction and those in the arc-continent collision in Taiwan region are different. In the northern Manila subduction zone, weak plate coupling creates the space together with positive buoyancy that facilitates the uplifting of the serpentinized materials. Otherwise, compressional force is the key factor to cause this phenomenon to be constrained in eastern Taiwan.

The transition from subduction of thinned continental lithosphere to full arc-continent collision left significant tectonic features of eastern Taiwan. Doo et al. (2015) have interpreted the uplifting serpentinized mantle rocks in the fore-arc region in the northern Manila subduction

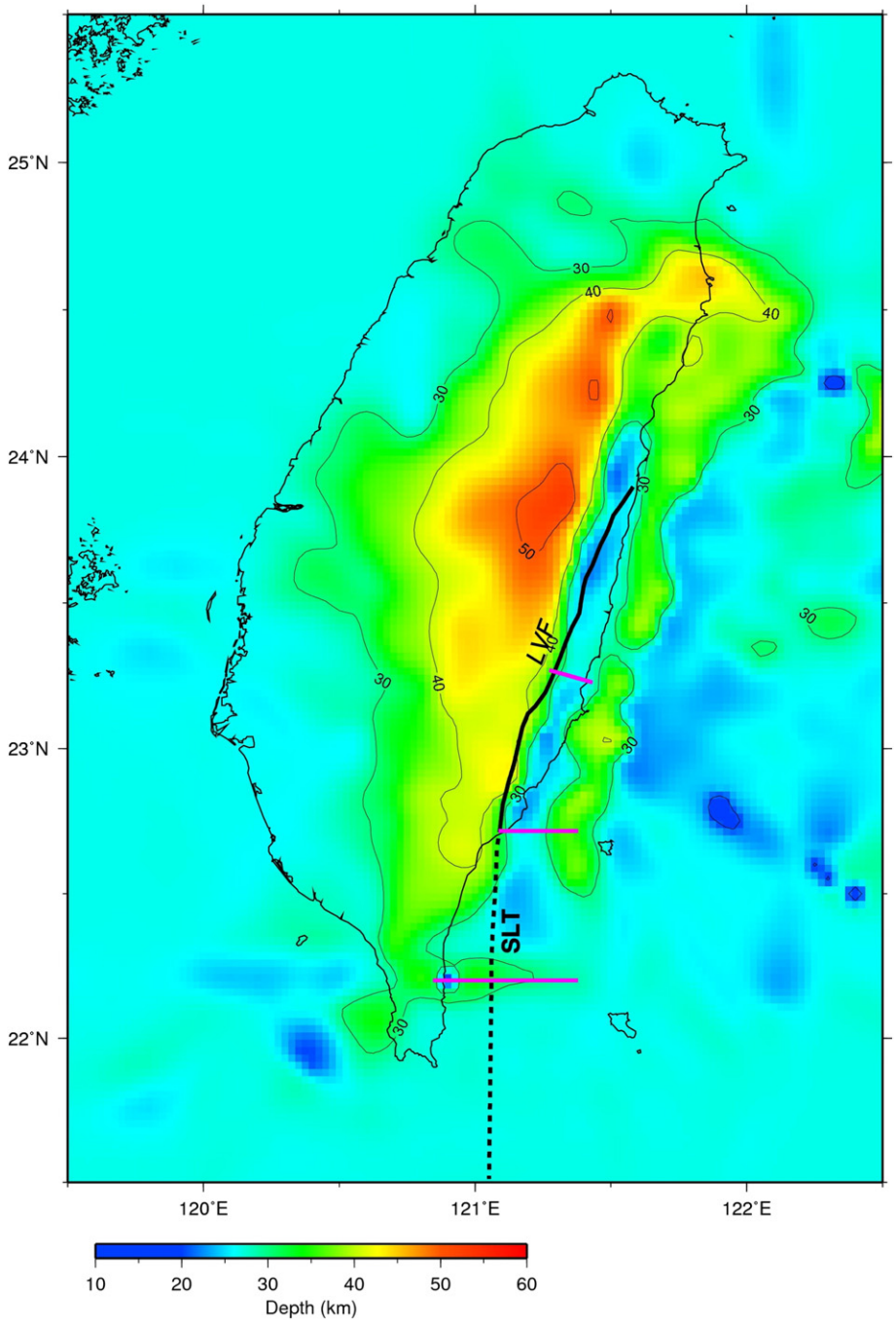

Fig. 6. The depths of the P-wave velocity 7.5 km/s isosurface from Kuo-Chen et al. (2012) velocity model. The presence of the high-velocity rise between the Eurasian Plate side and the Philippine Sea Plate side. Pink lines indicate the distributions of serpentinized materials. LVF: Longitudinal Valley Fault; SLT: southern Longitudinal trough.

zone. On the other hand, Van Avendonk et al. (2014) and our gravity modeling results as shown in this study suggest that this process also exists in eastern Taiwan. Considering the continuity of the convergent plate boundary between the South China Sea and the PSP, the integrated observation results from marine and onland studies show that the phenomenon of serpentinization of fore-arc mantle can be extended from the northern Manila subduction zone to onland eastern Taiwan (Fig. 5).

Acknowledgements

We thank Dr. Wu., F.T. for discussion and helpful comments. Wen-Bin Doo is supported by Ministry of Science and Technology of Taiwan (Grant No.: MOST 105-2611-M-008-002). D. Brown is funded by MINECO grant CGL2013-43877-P. Constructive reviews from Dr. T. Minshull and one anonymous reviewer are appreciated. Figures in this paper were generated using the generic mapping tools (GMT) (Wessel and Smith, 1998).

References

Beyssac, O., Negro, F., Simoes, M., Chan, Y.-C., Chen, Y.-G., 2008. High-pressure metamorphism in Taiwan: from oceanic subduction to arc-continent collision? Terra Nova 20, 118–125. http://dx.doi.org/10.1111/j.1365-3121.2008.00796.x.

Bostock, M.G., Hyndman, R.D., Rondenay, S., Peacock, S.M., 2002. An inverted continental Moho and serpentinization of the forearc mantle. Nature 147, 536–538. http://dx.doi.org/10.1038/417536a.

Brocher, T.M., 2005. Empirical relations between elastic wavespeeds and density in the Earth's crust. Bull. Seismol. Soc. Am. 95, 2081–2092. http://dx.doi.org/10.1785/0120050077.

Brown, D., Wu, Y.-M., Feng, K.-F., Chao, W.-A., Huang, H.-H., 2015. Imaging high-pressure rock exhumation in eastern Taiwan. Geology 43. http://dx.doi.org/10.1130/G36810.1.

Chen, P.-F., Huang, B.-S., Liang, W.-T., 2004. Evidence of a slab of subducted lithosphere beneath central Taiwan from seismic waveforms and travel times. Earth Planet. Sci. Lett. 229, 61–71. http://dx.doi.org/10.1016/j.epsl.2004.10.031.

Cheng, W.-B., 2009. Tomographic imaging of the convergent zone in Eastern Taiwan - a subducting forearc sliver revealed? Tectonophysics 466, 170–183. http://dx.doi.org/10.1016/j.tecto.2007.11.010.

Christensen, N., 1966. Elasticity of ultrabasic rocks. J. Geophys. Res. 71, 5921–5931. http://dx.doi.org/10.1029/JZ071i024p05921.

Christensen, N., 2004. Serpentinites, peridotites, and seismology. Int. Geol. Rev. 46, 759–816. http://dx.doi.org/10.2747/0020-6814.46.9.795.

Doo, W.-B., Lo, C.-L., Kuo-Chen, H., Brown, D., Hsu, S.-K., 2015. Exhumation of serpentinized peridotite in the northern Manila subduction zone inferred from forward gravity modeling. Geophys. Res. Lett. 42. http://dx.doi.org/10.1002/2015GL065705.

Erdman, M.E., Lee, C.Y.A., 2014. Oceanic-and continental-type metamorphic terranes: occurrence and exhumation mechanisms. Earth Sci. Rev. 139, 33–46. http://dx.doi.org/10.1016/j.earscirev.2014.08.012.

Gerya, T.V., 2011. Future directions in subduction modeling. J. Geodyn. 52, 344–378. http://dx.doi.org/10.1016/j.jog.2011.06.005.

Gerya, T.V., Stöckhert, B., Perchuk, A.L., 2002. Exhumation of high-pressure metamorphic rocks in a subduction channel: a numerical simulation. Tectonics 21. http://dx.doi.org/10.1029/2002TC001406.

Gvirtzman, Z., Nur, A., 1999. Plate detachment, asthenosphere upwelling, and topography across subduction zones. Geology 27, 563–566. http://dx.doi.org/10.1130/0091-7613(1999)027<0563:PDAUAT>2.3.CO;2.

Hacker, B.R., Gerya, T.V., 2013. Paradigms, new and old, for ultrahigh-pressure tectonism. Tectonophysics 603, 79–88. http://dx.doi.org/10.1016/j.tecto.2013.05.026.

Hacker, B.R., Aber, G.A., Peacock, S.M., 2003. Subduction factory 1. Theoretical mineralogy, densities, seismic wave speeds, and H2O contents. J. Geophys. Res. 108 (2029). http://dx.doi.org/10.1029/2001JB001127.

Hetland, E.A., Wu, F.T., 1998. Deformation of the Philippine Sea Plate under the Coastal Range, Taiwan: Results from an offshore-onshore seismic experiment. Terr. Atmos. Oceanic Sci. 9, 363–378.

Horen, H., Zamore, M., Dubuisson, G., 1996. Seismic waves velocities and anisotropy in serpentinized peridotites from Xigaze ophiolite: abundance of serpentine in slow spreading ridge. Geophys. Res. Lett. 23, 9–12. http://dx.doi.org/10.1029/95GL03594.

Huang, H.-H., Wu, Y.-M., Song, X., Chang, C.-H., Lee, S.-J., Chang, T.-M., Hsieh, H.-H., 2014. Joint Vp and Vs tomography of Taiwan: implications for subduction-collision orogeny. Earth Planet. Sci. Lett. 392, 177–191. http://dx.doi.org/10.1016/j.epsl.2014.02.026.

Hwang, C., Hsu, H.-J., Chang, T.Y., Featherstone, W.E., Tenzer, R., Lien, T., Hsiao, Y.-S., Shih, H.-C., Jai, P.-H., 2014. New free-air and Bouguer gravity fields of Taiwan from multiple platforms and sensors. Tectonophysics 611, 83–93. http://dx.doi.org/10.1016/j.tecto.2013.110.027.

Hyndman, R.D., Peacock, S.M., 2003. Serpentinization of the forearc mantle. Earth Planet. Sci. Lett. 212, 417–432. http://dx.doi.org/10.1016/S0012-821X(03)00263-2.

Kao, H., Jian, P.-R., 2001. Seismogenic patterns in the Taiwan region: insights from source parameter inversion of BATS data. Tectonophysics 333, 179–198. http://dx.doi.org/10.1016/S0040-1951(00)00274-2.

Kim, K.H., Chiu, J.-M., Pujol, J., Chen, K.-C., 2006. Polarity reversal of active plate boundary and elevated oceanic upper mantle beneath the collision suture in central eastern Taiwan. Bull. Seismol. Soc. Am. 96, 796–806. http://dx.doi.org/10.1785/0120050106.

Kuo-Chen, H., Wu, F.T., Roecker, S.W., 2012. Three-dimensional P velocity structures of the lithosphere beneath Taiwan from the analysis of TAIGER and related seismic data sets. J. Geophys. Res. 117, B06306. http://dx.doi.org/10.1029/2011JB009108.

Lin, C.-H., 2002. Active continental subduction and crustal exhumation: the Taiwan orogeny. Terra Nova 14, 281–287. http://dx.doi.org/10.1046/j.1365-3121.2002.00421.x.

Lin, C.-H., 2009. Compelling evidence of an aseismic slab beneath central Taiwan from a dense linear seismic array. Tectonophysics 466, 205–212. http://dx.doi.org/10.1016/j.tecto.2007.11.029.

Lin, C.-H., Yeh, Y.-H., Yen, H.-Y., Chen, K.-C., Huang, B.-S., Roecker, S., Chiu, J.-M., 1998. Three-dimensional elastic wave velocity structure of the Hualien region of Taiwan: evidence of active crustal exhumation. Tectonic 17, 89–103. http://dx.doi.org/10.1029/97TC02510.

Lo, C.-L., Doo, W.-B., Kuo-Chen, H., Hsu, S.-K., 2015. The buoyancy variation of plate coupling from subduction to collision: an example across the northernmost Manila trench. 2015 European Geosciences Union Vienna, Austria.

McIntosh, K.D., Nakamura, Y., Wang, T.-K., Shih, R.-C., Chen, A., Liu, C.-S., 2005. Crustal-scale seismic profiles across Taiwan and the western Philippine Sea. Tectonophysics 401, 23–54. http://dx.doi.org/10.1016/j.tecto.2005.02.015.

McIntosh, K., Van Avendonk, H., Lavier, L., Lester, W.R., Eakin, D., Wu, F., Liu, C.-S., Lee, C.-S., 2013. Inversion of a hyper-extended rifted margin in the southern Central Range of Taiwan. Geology 41, 871–874. http://dx.doi.org/10.1130/G34402.1.

Van Avendonk, H.J.A., Kuo-Chen, H., McIntosh, K.D., Lavier, L.L., Okaya, D.A., Wu, F.T., Wang, C.-Y., Lee, C.-S., Liu, C.-S., 2014. Deep crustal structure of an arc-continent collision: constraints from seismic traveltimes in central Taiwan and the Philippine Sea. J. Geophys. Res. 119. http://dx.doi.org/10.1002/2014JB011327.

Wang, H.-L., Zhu, L., Chen, H.-W., 2010. Moho depth variation in Taiwan from teleseismic receiver functions. J. Asian Earth Sci. 37, 286–291. http://dx.doi.org/10.1016/j.jseaes.2009.08.015.

Wu, Y.-M., Chang, C.-H., Zhao, L., Shyu, J.B.H., Chen, Y.-G., Sieh, K., Avouac, J.-P., 2007. Seismic tomography of Taiwan: improved constraints from a dense network of strong motion stations. J. Geophys. Res. 112, B08312. http://dx.doi.org/10.1029/2007JB004983.

Wu, F.T., Liang, W.-T., Lee, J.-C., Benz, H., Villasenor, A., 2009. A model for the termination of the Ryukyu subduction zone against Taiwan: a junction of collision, subduction/separation, and subduction bounsdaries. J. Geophys. Res. 114, B07404. http://dx.doi.org/10.1029/2008JB005950.

Xia, S., Sun, J., Huang, H., 2015. Degree of serpentinization in the forearc mantle wedge of Kyushu subduction zone: quantitative evaluations from seismic velocity. Mar. Geophys. Res. 36, 101–112. http://dx.doi.org/10.1007/s11001-014-9239-3.

Yu, S.-B., Kuo, L.-C., 2001. Present-day crustal motion along the Longitudinal Valley fault, eastern Taiwan. Tectonophysics 333, 199–217.

Yu, S.-B., Chen, H.-Y., Kuo, L.-C., 1997. Velocity of GPS stations in the Taiwan area. Tectonophysics 274, 41–59. http://dx.doi.org/10.1016/S0040-1951(96)00297-1.

Zhao, D., 2012. Tomography and dynamics of Western-Pacific subduction zones. Monogr. Environ. Earth Planets 1, 1–70.